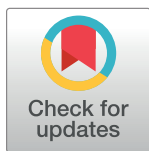


RESEARCH ARTICLE

The pathogenic biomarker alcohol dehydrogenase protein is involved in *Bacillus cereus* virulence and survival against host innate defence

Devon W. Kavanaugh , Constance Porrini , Rozenn Dervyn, Nalini Ramarao *

Micalis Institute, INRAE, AgroParisTech, Université Paris-Saclay, Jouy-en-Josas, France

* nalini.ramarao@inrae.fr

Abstract

Bacillus cereus is a spore forming bacteria recognized among the leading agents responsible for foodborne outbreaks in Europe. *B. cereus* is also gaining notoriety as an opportunistic human pathogen inducing local and systemic infections. The real incidence of such infection is likely underestimated and information on genetic and phenotypic characteristics of the incriminated strains is generally scarce. We have recently analyzed a large strain collection of varying pathogenic potential. Screening for biomarkers to differentiate among clinical and non-clinical strains, a gene encoding an alcohol dehydrogenase-like protein was identified among the leading candidates. This family of proteins has been demonstrated to be involved in the virulence of several bacterial species. The relevant gene was knocked out to elucidate its function with regards to resistance to host innate immune response, both *in vitro* and *in vivo*. Our results demonstrate that the *adhB* gene plays a significant role in resistance to nitric oxide and oxidative stress *in vitro*, as well as its pathogenic ability with regards to *in vivo* toxicity. These properties may explain the pathogenic potential of strains carrying this newly identified virulence factor.

OPEN ACCESS

Citation: Kavanaugh DW, Porrini C, Dervyn R, Ramarao N (2022) The pathogenic biomarker alcohol dehydrogenase protein is involved in *Bacillus cereus* virulence and survival against host innate defence. PLoS ONE 17(1): e0259386. <https://doi.org/10.1371/journal.pone.0259386>

Editor: Vijay Tripathi, Sam Higginbottom University of Agriculture, Technology and Sciences, INDIA

Received: May 25, 2021

Accepted: October 18, 2021

Published: January 4, 2022

Copyright: © 2022 Kavanaugh et al. This is an open access article distributed under the terms of the [Creative Commons Attribution License](https://creativecommons.org/licenses/by/4.0/), which permits unrestricted use, distribution, and reproduction in any medium, provided the original author and source are credited.

Data Availability Statement: All relevant data are within the manuscript.

Funding: The author(s) received no specific funding for this work.

Competing interests: The authors have declared that no competing interests exist.

Introduction

Bacillus cereus is an ubiquitous spore forming human pathogen. It is present in soil, foods, almost all surfaces in hospital settings, and human skin. It is the second leading cause of collective foodborne outbreaks in France after *Staphylococcus aureus* and the third in Europe [1–3]. *B. cereus* was associated with 155 outbreaks, 1,636 illnesses and 44 hospitalizations in Europe in 2019 according to reports by 27-member states. *B. cereus* can induce two types of gastrointestinal diseases, leading to emetic or diarrhoeal syndromes. *B. cereus* can also cause severe systemic infections, especially in immunocompromised patients leading to patient death in approximately 10% of cases [4–9]. However, some *B. cereus* strains can cause severe and even fatal infections in healthy people [10]. The pathogenic potential of *B. cereus* is thus extremely variable, with some strains being harmless and others lethal [11].

B. cereus produces toxins such as Hbl, Nhe, and CytK that induce cell toxicity [12–14]. In addition, other factors such as HlyII, InhA1, CwpFM or Mfd have been implicated in *B. cereus* resistance against the host immune system [15–21]. These toxins provide an indication of the strain toxicity potential [13, 22–24]. However, these factors do not allow the discrimination of strains according to their pathogenicity. Indeed, several studies have shown that the Nhe production by hazardous strains is variable and that non-pathogenic strains can also produce it in large quantities [1, 24]. Moreover, these toxins do not appear to be suitable markers for strains causing non-gastrointestinal infections [22].

B. cereus strains that induced severe gastrointestinal or non-gastrointestinal disorders do not carry neither *hbl*, *ces*, *hlyII*, *cytK1* nor *cytK2* genes and did not produce the Nhe protein, implying that other still unknown factors were responsible for their pathogenicity [1, 11].

Accordingly, we have recently analyzed a large strain collection comparing strains that induced an infection (intestinal or otherwise) with non-pathogenic strains [11, 25]. The large strain screening allowed to identify a combination of four as yet undescribed biomarkers, wherein their presence/absence allows an accurate identification of clinical *B. cereus* strains [26]. Three of these genes are located on the bacterial chromosome, and the fourth one is located on a large plasmid in a region that could be defined as a novel pathogenicity island for *B. cereus* [27]. These findings constitute a huge step in the understanding of the *B. cereus* pathogenic potential and complexity and may provide tools to better assess the risks associated with *B. cereus* contamination. Among these genes, *adhB*, was identified as a leading candidate [26]. This *adhB* gene encodes an alcohol dehydrogenase-like protein (ADH). This family of enzymes is involved in oxidation-reduction biological process. ADH are involved in metabolic and physiological processes in a variety of organisms, including fermentative metabolism [28], the oxidation of alcohols as carbon and energy sources [29], protection against anaerobic stress [30], and maintenance of the intracellular redox balance [31].

In this study, the *adhB* gene was knocked out to better elucidate its function during *B. cereus* virulence. Our results demonstrate that *adhB* plays a significant role in resistance to nitric oxide (NO) and oxidative stress *in vitro*, as well as its pathogenic ability with regards to *in vivo* infection and toxicity. These properties may explain the pathogenic potential of strains carrying this newly identified virulence factor.

Materials and methods

Bacterial strains

This study includes 35 *B. cereus* strains isolated from human patients following systemic or local infections and 21 non-pathogenic strains (Table 1). The 35 strains of the clinical collection were isolated from patient samples (biopsy, blood culture, etc) from nine French voluntary hospitals between 2008 and 2014. The samples and information were collected for a previous study and were treated anonymously and thus not subjected to personal consent [22]. The non-pathogenic strains have been isolated from food, where no infection was reported in humans. They were further tested in cell and animal models and did not induce any pathologies [23, 25]. We have previously shown a correlation between cytotoxicity and virulence [11]. Nevertheless, although these strains had previously been shown to be weakly cytotoxic to human cells and to have reduced virulence in an insect infection model, this does not rule out their potential ability to produce symptoms in specific vulnerable populations (i.e. the elderly, immunocompromised, or premature/new-born babies).

Table 1. Characteristics of non-pathogenic (A) and clinical (B) strains.

A					
Non-pathogenic strains	Source	adhB			
INRA-PF_S09	Milk protein	0			
I13_S10	Cooked rice	1			
INRA-5_S11	Pasteurized zucchini puree	0			
INRA-C64_S12	Pasteurized vegetables	0			
ADRIA-I3_S13	Cooked foods	0			
INRA-BN_S36	Vegetable	1			
INRA-PA_S37	Milk protein	0			
INRA-A3_S38	Starch	1			
I23_S39	Cooked apple	0			
SB_S40	Soil from a vegetable field	0			
I11_S41	Cooked food	1			
INRA-C1_S42	Pasteurized vegetables	0			
INRA-C46_S43	Pasteurized vegetables	0			
INRA-SL_S44	Soil	0			
INRA-SO_S45	Soil	0			
INRA-BC_S47	Vegetable	1			
I2_S48	Dried fruit	0			
INRA-BL_S49	Vegetable	0			
ADRIA I21_S50	Cooked foods	0			
INRA-SV_S51	Soil	0			
WSBC 10204_S52	Pasteurized milk	0			
B					
Clinical strains	Age of patients	Type of sampling	Symptoms	Outcomes	adhB
09CEB13BAC_S6	Premature newborn	Blood culture	Brain abscess	Recovery	1
09CEB14BAC_S7	Premature newborn	Blood culture	Bacteremia	Recovery	1
09CEB33BAC_S8	Newborn	Axilla-later feces	Skin infection	Recovery	1
12CEB31BAC_S14	Premature newborn	Blood culture	Organ failure and pulmonary and cerebral abscesses	Death	1
13CEB06BAC_S15	86	Blood culture from catheter	Heart failure, ventilator-associated pneumonia, ischemic stroke	Recovery	1
09CEB11BAC_S16	Premature newborn	Blood culture	Meningitis, infection in the liver, both lungs	Death	1
09CEB16BAC_S17	Newborn	Umbilical	Local colonization	Recovery	1
12CEB30BAC_S18	Premature newborn	Blood culture	Sepsis	Recovery	1
12CEB40BAC_S20	63	Blood culture	Bacteremia and central venous catheter-linked infection	Recovery	1
12CEB46BAC_S21	61	Blood culture	Sepsis (patient with an acute myeloid leukemia)	Recovery	1
12CEB47BAC_S22	43	Blood culture	Bacteremia	Recovery	1
12CEB51BAC_S23	60	blood culture	Sternum abscess, absent fever	Sequela of osteitis	1
13CEB01BAC_S24	31	Prosthesis from tibia	No clinical sign of infection	Recovery	1
09CEB12BAC_S53	Premature newborn	Cerebrospinal fluid	Meningitis, infection in the liver, both lungs	Death	1
09CEB34BAC_S59	Premature-newborn	Stomach-tube feeding	Premature birth	Recovery	1
09CEB36BAC_S61	Premature-newborn	Central venous catheter	Bacteremia	Recovery	1

(Continued)

Table 1. (Continued)

12CEB34BAC_S64	80	Thoracentesis	Pulmonary infection	not known	1
12CEB37BAC_S90	30	Blood culture	Endocarditis	Death	1
12CEB38BAC_S91	65	Blood culture	Sepsis	Death	1
12CEB39BAC_S92	54	Blood culture	Sepsis	Recovery	1
12CEB42BAC_S94	63	Blood culture	Bacteremia and central venous catheter-linked infection	Recovery	1
12CEB43BAC_S95	63	Blood culture	Bacteremia and central venous catheter-linked infection	Recovery	1
12CEB44BAC_S96	34	Blood culture	Bacteremia	Recovery	1
12CEB45BAC_S97	newborn	Blood culture	Kidneys and urinary infections	Recovery	1
12CEB48BAC_S98	66	Blood culture	Bacteremia (patient with a colorectal cancer)	Recovery	1
12CEB49BAC_S99	24	Blood culture+ skin infection	Sepsis and aplastic anemia caused by drugs	Recovery	1
12CEB50BAC_S100	77	Blood culture	Bacteremia (patient with breast cancer)	Recovery	1
12CEB52BAC_S101	40	Blood culture	Bacteremia (immunocompromised patient)	Recovery	0
13CEB03BAC_S102	76	Blood culture	Community acquired pneumonia	Recovery	1
13CEB07BAC_S105	24	Blood culture	Abdominal pain, shivering, vomiting, fever, diarrhea	Recovery	1
13CEB09BAC_S106	85	Liver abscess	Sepsis, hepatitis c and liver abscess, abdominal pain, diarrhea	Recovery	1
13CEB30BAC_S107	not known	Blood culture	Nausea, abdominal pain and vomiting	not known	1
14CEB16BAC_S114	Premature newborn	Blood culture from peripheral veins	Septic shock, multiple organ failure, pulmonary and cerebral abscesses	Death	1
14CEB17BAC_S115	Premature newborn	Bronchial aspiration (lung)	Septic shock and pneumonia pulmonary necrotic abscesses, recurrent pneumothorax	Death	1
14SBCL987_S116	not known	Biopsy (kidney)	Vomiting and diarrhea	Death	1

The absence (0) or presence (1) of the *adhB* gene was detected by PCR.

<https://doi.org/10.1371/journal.pone.0259386.t001>

adhB gene detection by PCR

For all the strains, a single colony was picked, resuspended in 100 μ L Tris-EDTA NaCl buffer (TEN) and incubated at 98°C for 10 min. After centrifugation to pellet cell debris, 1 μ L of supernatant was used as DNA matrix. The PCR mixture for gene detection contained 1 μ L DNA matrix, 0.5 μ M primer (forward: TTATTATCTATTCTTTTCGTGTGATGC, and reverse CTATTTGTAGCAGAACATTCRAAACC), 10 μ L DreamTaq Green PCR Master Mix (2X) (Thermo Scientific) in a final volume of 20 μ L. Thermal cycling was carried out in a Mastercycler[®] nexus (Eppendorf) with the following program: a start cycle of 3 min at 98°C, followed by 30 cycles of 20 s at 98°C, 30 s at 55°C, and 1 min at 72°C, and a final extension time of 10 min at 72°C. PCR fragment sizes were revealed on 1.5% agarose gels containing Midori Green, and visualised by a UV imaging device as previously described [26].

adhB mutant generation

The Bt407 Cry⁻ with the reference genome *Bacillus thuringiensis* Bt407: NC_018877.1 was used as a model for *B. cereus* and was renamed Bc 407.

Knock-out of the *adhB* gene (WP_000438843) was accomplished by double-cross over gene substitution by use of the pMAD vector [32]. Briefly, using the available sequencing information of the Bc407 strain, 600 bp regions upstream and downstream of the identified gene of interest were synthesized surrounding a tetracycline-resistance cassette by the GeneCust company (Boynes, France). The upstream nucleotide coordinates used are 2,575,680 to 2,576,279, and the downstream nucleotide coordinates are 2,577,204 to 2,577,802. The synthesized region was then ligated into the pMAD vector. This vector was further transformed by heat shock into chemically competent NEB-10 beta cells. The plasmid was then extracted and transformed

into *E. coli* strain ET to facilitate de-methylation of the plasmid, increasing subsequent transformation into *B. cereus* Bc407 as previously described [16]. Resulting colonies were then subjected to temperature stress at 40°C to force the incorporation of the resistance cassette leading to the stable knock-out of the *adhB* gene, which was verified by PCR with oligonucleotide sequences flanking the cloned region. The mutation was stable and sequencing revealed that the mutation occurred at the corrected place and did not affect the flanking regions. The resulting strain was designated as $\Delta adhB$.

Wild type and mutant strains were streaked onto BHI agar from 20% glycerol stocks to obtain isolated colonies. Colonies were inoculated into BHI broth and grown at 37°C, 200 rpm until mid to late-exponential phase for phenotypic analysis. Cultures in mid-exponential phase were used for microscopy to determine cellular morphology. For growth assays, stocks were inoculated into BHI broth and followed by sampling for CFU/ml at regular intervals.

Nitric oxide (NO) stress survival

B. cereus Bc407 and the $\Delta adhB$ mutant were grown to late-exponential phase. Cultures were harvested and diluted 1:1000 in RPMI (Gibco Glutamax, Fisher Scientific, Illkirch Cedex, France) and further grown at 37°C without agitation with differing doses of the NO donor, NOC-5 (3-[2-hydroxy-1-(1-methylethyl)-2-nitrosohydrazino]-1-propanamine (Calbiochem, Sigma-Aldrich, Saint-Louis, MO, USA). NOC-5 was dissolved in NaOH 0.01 M and used at the following concentrations: 0, 15.6, 25, 31.25, 50, 62.5, 100, 125, 250, 500 μ M. After 1 h, bacteria were agitated to avoid sedimentation and the survival rate was quantified after 4 h by plating serial dilutions on LB agar plates. Data are pooled from two to four independent experiments and presented as % survival = (NO-treated/Buffer-treated) \times 100.

Oxidative stress survival

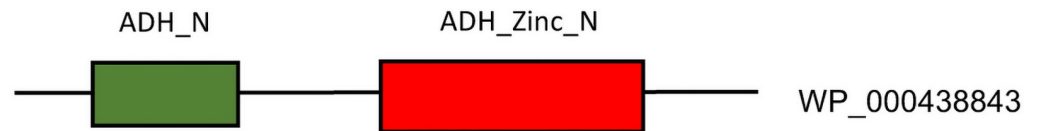
Oxidative stress-resistance was determined as previously described [33]. Briefly, wild-type and $\Delta adhB$ mutant strains were grown and 2 h post-inoculation, 500 μ l of each culture was added to 100 μ l of either sterile water or hydrogen peroxide at final concentrations of 2 mM or 10 mM. Treated (2 mM or 10 mM H₂O₂) and control (H₂O) cultures were incubated for 10 min at 37°C and then serially diluted in phosphate-buffered saline (PBS) and plated on BHI to stop the reaction and count CFU/ml. Data are pooled from two independent experiments and presented as % survival = (H₂O₂-treated/H₂O-treated) \times 100.

Insect infection trial

B. cereus Bc407 and the $\Delta adhB$ mutant were grown to exponential phase. Cultures were harvested and serially diluted 1:4 in peptone water prior to injection. 10 to 20 last instar *Galleria mellonella* larvae were used following a 24 h fast as previously described [34, 35]. 10 μ l of bacterial preparations at various doses were injected between the second and third body segment from the rear of the insect. Injected insects were incubated at 37°C for 24 h, following which survival was assessed. Peptone water was injected as negative control. Data are pooled from three independent experiments and presented as % survival = (injected with strain/injected with water) \times 100.

Protein bioinformatic analysis

The protein sequences of the ADH protein (WP_000438843) was analysed with Pfam to find functional domains. E-values are based on searching the Pfam-A family against UniProtKB 2018_04 using HMM search.



Domain	Start	End	Gathering threshold (bits)		Score (bits)		E-value	
			Sequence	Domain	Sequence	Domain	Sequence	Domain
ADH_N	26	91	21.10	21.10	33.90	25.10	0.00015	0.079
ADH_zinc_N	147	265	31.80	31.80	33.30	32.60	0.00025	0.00042

Fig 1. Structural domains of AdhB. The AdhB protein of *B. cereus* is composed of a catalytic domain with an inserted zinc-binding domain (green box) and a co-factor-binding domain at its C terminus (red box). E-values are based on searching the Pfam-A family against UniProtKB 2018_04 using hmmsearch.

<https://doi.org/10.1371/journal.pone.0259386.g001>

Statistical analysis

Statistical analysis was performed with GraphPad Prism version 7. Insect survival curves were assessed by non-linear regression, constraining the bottom to 0.

Bacterial survival rate following stresses were also analysed by non-linear regression, and the statistical differences were calculated with a Wilcoxon test between the conditions with or without stress.

Results

adhB as a marker of clinical *B. cereus* strains

The presence/absence of the *adhB* gene was assessed by PCR on a collection of strains of varying pathogenic potential: 21 non-pathogenic strains and 35 clinical strains (Table 1). *adhB* was present in 34/35 (97%) clinical isolates, whereas it was present in 5 of 21 (24%) non-pathogenic isolates. We thus hypothesised that *adhB* may be a new and important virulence factor of *B. cereus*.

The amino acid sequences of the Bc407 gene WP_000438843 coding for a protein of the AdhB family was analysed using the Uniprot database (Fig 1). This enzyme of 308 amino acids belongs to the zinc-containing alcohol dehydrogenase family. The software identified two domains, with the catalytic domain of the alcohol dehydrogenase containing an inserted zinc-binding domain. This domain has a GroES-like structure [36, 37]. The co-factor-binding domain of the enzyme is located proximal to the C-terminus. Structural studies indicate that it forms a classical motif called Rossmann fold that reversibly binds NAD(H) as a co-factor [38, 39].

Growth characteristics and morphology

B. cereus Bc407 and the $\Delta adhB$ mutant were grown in BHI medium at 37°C, 200 rpm and bacterial growth was followed by measuring the OD₆₀₀, and CFU/mL determined by serial dilution and plating (Fig 2A and 2B). The two strains presented similar rates of growth with no significant differences in growth curves. The strains were observed under the microscope and bacterial morphology shows that the two strains are similar in cellular shape and size, with the *adhB* mutant often making longer chains of cells (6–8 cells) (Fig 2C and 2D).

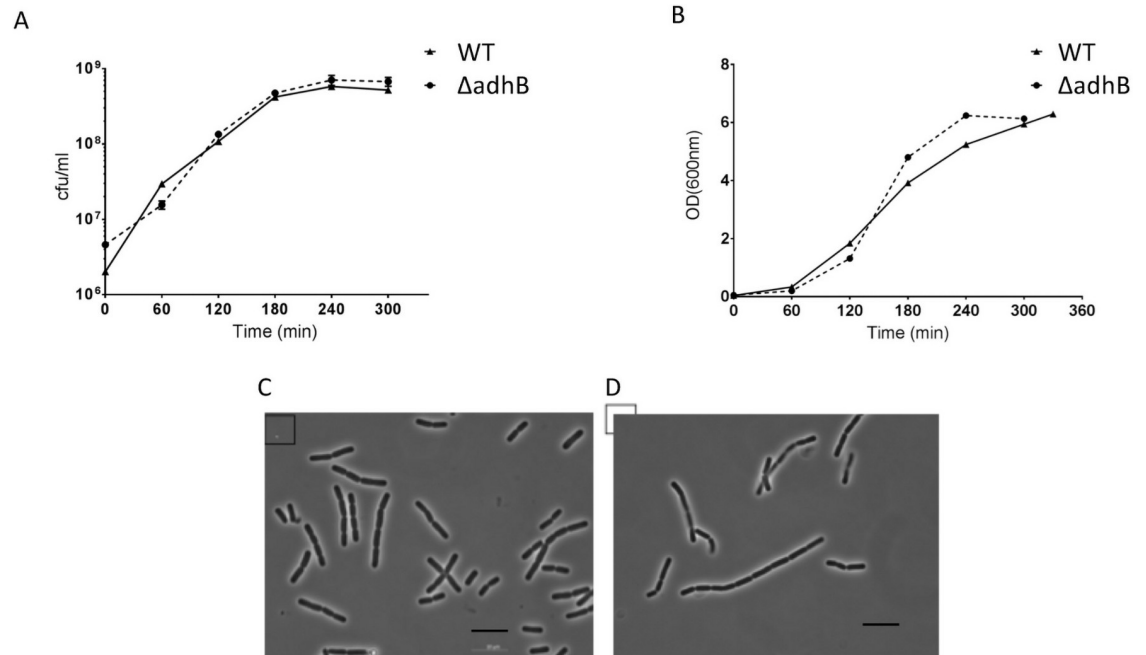


Fig 2. Bacterial growth curves and cellular morphology. Bacterial growth was determined by calculating CFU/mL (A) or following optical density at 600 nm (B) for the wildtype *B. cereus* Bc407 (▲; solid line) and the $\Delta adhB$ mutant (●; dashed line) strains. Representative bacterial morphology of Bt407 WT (C) and *adhB* mutant (D) are viewed at 100x magnification. The scale bar represents a length of 10 μ m. All graphs represent one representative experiment out of three biological replicates.

<https://doi.org/10.1371/journal.pone.0259386.g002>

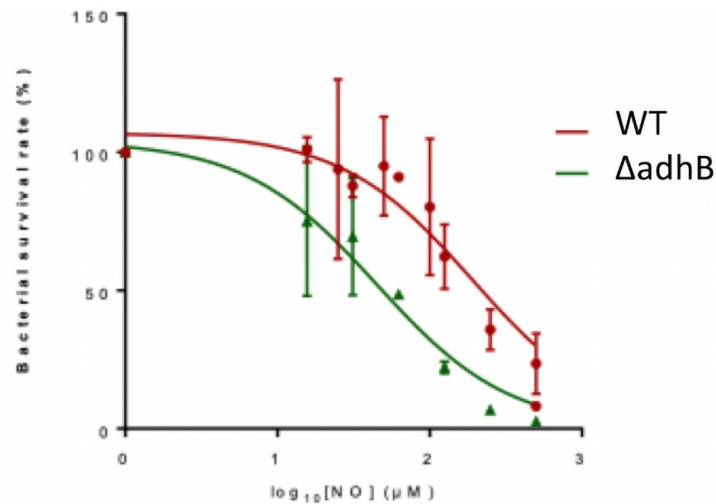
Nitric oxide (NO) and oxidative stress resistance

To assess the role of AdhB in the resistance to the host immune system response, *B. cereus* Bc407 and $\Delta adhB$ strains were incubated with the NO donor to test their resistance against NO stress (Fig 3). Several doses of NO were assessed and the dose inhibiting 50% of bacterial growth (IC₅₀) was calculated. The IC₅₀ of *B. cereus* wild type (WT) strain is approximately 4 times higher than that of the mutant (193 vs 45 μ M of NO) and the survival rate of the mutant is lower at each concentration of NO tested. Thus, the mutant *adhB* is more sensitive to nitric oxide than the wild type strain.

Then, oxidative stress resistance of *B. cereus* Bc407 WT and $\Delta adhB$ strains was determined after exposure to 2 mM or 10 mM H₂O₂ for 10 min at 37°C (Fig 4). Wildtype Bc407 demonstrated increased resistance at both concentrations, with survival percentage being 14-fold higher at 2 mM, and 20-fold higher at 10 mM.

Insect model of *B. cereus* toxicity

The role of AdhB in the pathogenicity of *B. cereus* was assessed in an insect model of infection. *B. cereus* Bc407 and $\Delta adhB$ mutant strains were injected at various doses into *Galleria mellonella* larvae (Fig 5). At 24 h post-injection, survival of the insects was assessed. Insects infected with the $\Delta adhB$ mutant strain demonstrated higher rates of survival in relation to the wildtype strain, demonstrating a reduced virulence of the mutant strain. Further, statistical analysis of the survival curves reveals a significant difference in the LD₅₀ values between the strains: 4.2 10^3 CFU/injection for the wildtype and 1.5 10^4 CFU/injection for the $\Delta adhB$ mutant. HillSlope determined the curves to be distinct at 99.94% probability.



	<i>B. cereus</i> Bc407 WT	<i>B. cereus</i> Bc407 ΔadhB
IC50	193 µM	45 µM

Fig 3. NO sensitivity. The wild type and $\Delta adhB$ mutant strains were cultured and incubated for 4 h in the presence of different concentrations of NO donors. Bacterial survival was quantified by plating and bacterial resistance to NO was measured and normalized with respect to the control condition, without NO. Data points correspond to the mean \pm SEM of the values obtained from 2 to 4 biological replicates. The calculation of the IC50 of NO was performed using Graphpad.

<https://doi.org/10.1371/journal.pone.0259386.g003>

Discussion

Alcohol dehydrogenase (ADH) is an enzyme involved in oxidation-reduction biological process. It catalyses the reversible oxidation of alcohols and induces the formation of their corresponding acetaldehyde or ketone with the reduction of NAD (Fig 6). This class of enzyme typically has a broad spectrum of action [40, 41]. Here we characterized AdhB as a protein involved in *B. cereus* resistance to nitric and oxidative stresses, two major components of the host immune system, and in its pathogenicity.

Currently three types of alcohol dehydrogenases are known, that differ structurally and catalytically: Zinc-containing 'long-chain' alcohol dehydrogenases, 'short-chain' alcohol dehydrogenases, and iron-containing alcohol dehydrogenases [42, 43]. The AdhB (WP_000438843) protein in *B. cereus* is a zinc-containing ADH. These enzymes are typically dimeric or tetrameric proteins, which require two atoms of zinc per subunit to be functional, however, catalytic activity is maintained in the presence of a single zinc atom. The zinc atoms interact with either cysteine or histidine residues; the catalytic zinc being coordinated by two cysteines and one histidine. Zinc-containing ADH's are found in bacteria, mammals, plants, and fungi. Normally, there is more than one isozyme per species (e.g. humans possess at least six isozymes and yeast have three). Consistently, we identified three Zinc-containing ADH's in the Bc407 strain (WP_000438843, WP_000649129.1, WP_000645827.1). These three isozymes share common structures with two identified domains (not shown). The first is the catalytic domain that might contain an inserted zinc-binding domain. This domain has a GroES-like structure; a name derived from the superfamily of proteins with a GroES fold. Proteins with a GroES fold structure have a highly conserved hydrophobic core and a glycyl-aspartate dipeptide,

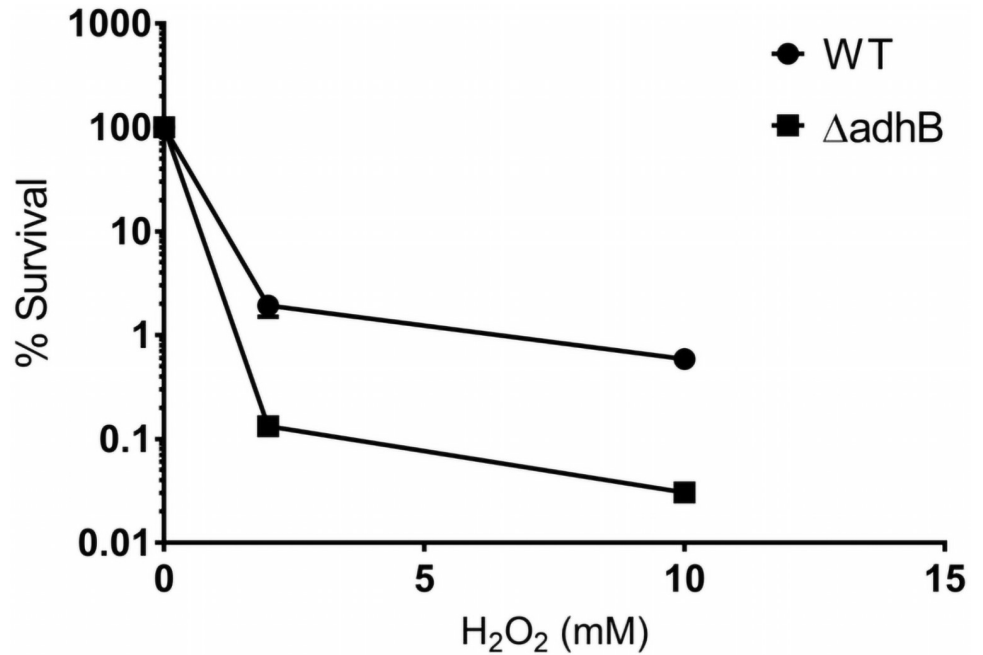
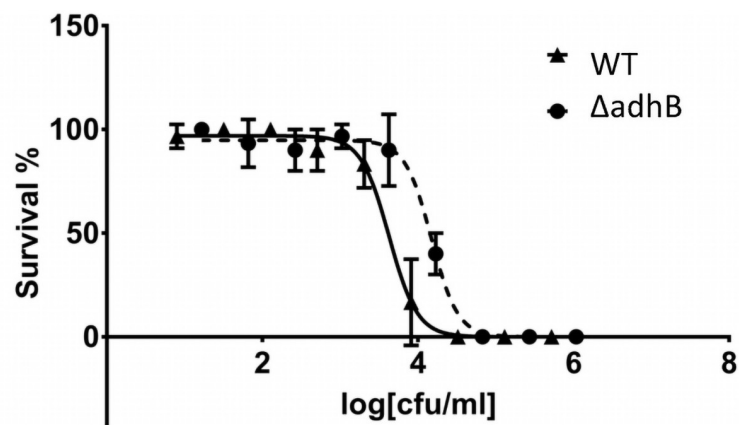


Fig 4. H₂O₂ sensitivity. The wild-type and $\Delta adhB$ mutant strains were grown and subsequently exposed to either 2 mM or 10 mM of hydrogen peroxide for 10 min at 37°C. Bacterial survival was assessed by plating and normalized against buffer-treated controls. Data points correspond to the mean \pm SEM of the values obtained from 2 biological replicates.

<https://doi.org/10.1371/journal.pone.0259386.g004>



	<i>B. cereus</i> Bc407 WT	<i>B. cereus</i> Bc407 $\Delta adhB$
LD50	4.2 10 ³ cfu/injection	1.5 10 ⁴ cfu/injection

Fig 5. Insect infection. Bacterial virulence was determined as *Galleria mellonella* survival percentage following injection with varying CFU/mL of wild type (triangles, black line) or $\Delta adhB$ (circles, dashed line) mutant strains. Survival was measured as live insects following 24 h post-injection. Calculation of the LD50 was done using Graphpad software.

<https://doi.org/10.1371/journal.pone.0259386.g005>

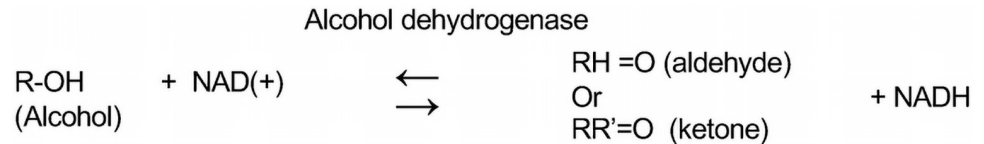


Fig 6. Reaction catalyzed by an alcohol dehydrogenase. The alcohol dehydrogenase catalyzes the oxidation of alcohol into their corresponding aldehyde (primary alcohol) or ketone (secondary alcohol) with the reduction of NAD+.

<https://doi.org/10.1371/journal.pone.0259386.g006>

which is thought to maintain the fold. The second is the domain that binds its cofactor NAD owing to its motif denoted as a Rossmann fold [38, 39].

In order to specify the role of AdhB in *B. cereus*, the virulence of the wild type and $\Delta adhB$ mutant was tested in an insect infection model. *G. mellonella* larvae were used as a model of infection as *B. cereus* is both a human and an insect pathogen [25, 44]. This study reveals that *adhB* plays an essential role during *B. cereus* virulence and could thus be considered as a new pathogenic factor.

During human or insect infections, *B. cereus* is able to resist the host immune system and persist. It can indeed survive phagocytosis by macrophages and can induce their apoptosis [20, 45]. The primary mechanism of macrophage-induced cytotoxicity is through the massive production of nitric oxide and oxidative stress at the peak of inflammation leading to bacterial death [46, 47]. Thus, bacterial response to NO is of major importance for bacterial survival and several pathogenic bacteria have developed means for detoxification and repair of the damages caused by NO [48]. We have previously shown that *B. cereus* is particularly resistant to NO [15, 18, 45, 49]. Here, we show that the $\Delta adhB$ mutant was more sensitive than the wild-type strain to both oxidative and nitric stresses. Accordingly, this sensitivity may be implicated in the reduced mutant virulence in the insect model.

The initial step of bacterial response to NO and oxidative response is the detection of reactive oxygen and nitrogen species (ROS and RNS), which will permit to activate the detoxification and repair pathways. It has been previously shown that virulence factor production by *B. cereus* is dynamic and shaped by cellular oxidation [50]. ADH proteins have been previously shown to be involved in the reduction of alcohol and the production of NADH. NADPH is required to maintain and regenerate the cellular detoxifying and anti-oxidative defense systems [51]. The antioxidant defense system of *B. cereus* is constituted by an elaborate, often overlapping network of enzymes [52], but to the best of our knowledge, there was no evidence of ADH implication in the resistance of oxidative or NO stress. As oxidative and NO response overlap during the immune response, it is not surprising that mechanisms of bacterial resistance against ROS and RNS share similarities. The reduction capacity of ADH may be involved in NO detoxification. Bacterial capacity to detoxify NO through reduction is widely distributed in denitrifying bacteria but is also present in pathogens. For denitrifying bacteria, the reduction of nitrate to N₂ is part of the nitrogen cycle and prevents NO high toxicity; for pathogenic bacteria, NO detoxification might be a mean to survive under oxygen limited environments and to survive to nitrogen stress [46, 47, 53].

Taken together, we have identified a new virulence factor implicated in *B. cereus* resistance to host immunity whose activities may explain the pathogenic potential of clinical strains carrying this newly identified pathogenic biomarker.

Author Contributions

Conceptualization: Nalini Ramarao.

Formal analysis: Devon W. Kavanaugh, Nalini Ramarao.

Funding acquisition: Nalini Ramarao.

Methodology: Devon W. Kavanaugh, Constance Porrini, Rozenn Dervyn, Nalini Ramarao.

Project administration: Nalini Ramarao.

Supervision: Nalini Ramarao.

Writing – original draft: Devon W. Kavanaugh, Constance Porrini.

Writing – review & editing: Nalini Ramarao.

References

1. Glasset B, Herbin S, Guiller L, Cadel-Six S, Vignaud ML, Grout J, et al. Large-scale survey of *Bacillus cereus*-induced food-borne outbreaks: epidemiologic and genetic characterization EuroSurveillance. 2016; 21(48): 30413.
2. Stenfors Arnesen L, Fagerlund A, Granum P. From soil to gut: *Bacillus cereus* and its food poisoning toxins. FEMS Microbiol Rev. 2008; 32:579–606. <https://doi.org/10.1111/j.1574-6976.2008.00112.x> PMID: 18422617
3. Ramarao N, Lereclus D, Sorokin A. The *Bacillus cereus* group. Molecular Medical Microbiology. 2015; III(Second Edition):1041–78.
4. Veyssyre F, Fourcade C, Lavigne JP, Sotto A. *Bacillus cereus* infection: 57 case patients and a literature review. Med Mal Infect. 2015; 45(11–12):436–40. Epub 2015/11/04. <https://doi.org/10.1016/j.medmal.2015.09.011> PMID: 26525185
5. Bottone EJ. *Bacillus cereus*, a volatile human pathogen. Clin Microbiol Rev. 2010; 23(2):382–98. <https://doi.org/10.1128/CMR.00073-09> PMID: 20375358
6. Ramarao N, Belotti L, Deboscker S, Ennahar-Vuillemin M, de Launay J, Lavigne T, et al. Two unrelated episodes of *Bacillus cereus* bacteremia in a neonatal intensive care unit. Am J Infect Control. 2014; 42(6):694–5. <https://doi.org/10.1016/j.ajic.2014.01.025> PMID: 24725514
7. Gaur AH, Patrick CC, McCullers JA, Flynn PM, Pearson TA, Razzouk BI, et al. *Bacillus cereus* bacteremia and meningitis in immunocompromised children. Clin Infect Dis. 2001; 32:1456–62. <https://doi.org/10.1086/320154> PMID: 11317247
8. Lotte R, Herisse AL, Berrouane Y, Lotte L, Casagrande F, Landraud L, et al. Virulence Analysis of *Bacillus cereus* Isolated after Death of Preterm Neonates, Nice, France, 2013. Emerg Infect Dis. 2017; 23(5):845–8. <https://doi.org/10.3201/eid2305.161788> PMID: 28418291
9. Cormontagne D, Rigourd V, Vidic J, Rizzotto F, Bille E, Ramarao N. *Bacillus cereus* Induces Severe Infections in Preterm Neonates: Implication at the Hospital and Human Milk Bank Level. Toxins (Basel). 2021; 13(2). <https://doi.org/10.3390/toxins13020123> PMID: 33562185
10. Hoffmaster AR, Hill KK, Gee JE, Marston CK, De BK, Popovic T, et al. Characterization of *Bacillus cereus* isolates associated with fatal pneumonias: strains are closely related to *Bacillus anthracis* and harbor *B. anthracis* virulence genes. J Clin Microbiol. 2006; 44(9):3352–60. 44/9/3352. <https://doi.org/10.1128/JCM.00561-06> PMID: 16954272
11. Glasset B, Sperry M, Dervyn R, Herbin S, Brisabois A, Ramarao N. The cytotoxic potential of *Bacillus cereus* strains of various origins. Food Microbiol. 2021; 98:103759. <https://doi.org/10.1016/j.fm.2021.103759> PMID: 33875199
12. Fagerlund A, Lindbäck T, Storset A, Granum P, Hardy S. *Bacillus cereus* Nhe is a pore forming toxin with structural and functional properties similar to ClyA (HlyE, SheA) family of haemolysins, able to induce osmotic lysis in epithelia. Microbiol. 2008; 154:693–704. <https://doi.org/10.1099/mic.0.2007/014134-0> PMID: 18310016
13. Ramarao N, Tran SL, Marin M, Vidic J. Advanced Methods for Detection of *Bacillus cereus* and Its Pathogenic Factors. Sensors (Basel). 2020; 20(9). <https://doi.org/10.3390/s20092667> PMID: 32392794
14. Guinebretière MH, Thompson, Sorokin A, Normand P., Dawyndt P., Ehling-Schulz M, et al. Ecological diversification in the *Bacillus cereus* Group. Environ Microbiol. 2008; 10:851–65. <https://doi.org/10.1111/j.1462-2920.2007.01495.x> PMID: 18036180
15. Darrigo C, Guillemet E, Dervyn R, Ramarao N. The Bacterial Mfd Protein Prevents DNA Damage Induced by the Host Nitrogen Immune Response in a NER-Independent but RecBC-Dependent Pathway. PLoS ONE. 2016; 11(10):e0163321. <https://doi.org/10.1371/journal.pone.0163321> PMID: 27711223

16. Guillemet E, Cadot C, Tran SL, Guinebretiere MH, Lereclus D, Ramarao N. The InhA metalloproteases of *Bacillus cereus* contribute concomitantly to virulence. *J Bacteriol.* 2010; 192(1):286–94. <https://doi.org/10.1128/JB.00264-09> PMID: 19837797.
17. Haydar A, Tran SL, Guillemet E, Darrigo C, Perchat S, Lereclus D, et al. InhA1-Mediated Cleavage of the Metalloprotease NprA Allows *Bacillus cereus* to Escape From Macrophages *Front Microbiol.* 2018; 23:1063. <https://doi.org/10.3389/fmicb.2018.01063> PMID: 29875760
18. Guillemet E, Lereec A, Tran SL, Royer C, Barbosa I, Sansonetti P, et al. The bacterial DNA repair protein Mfd confers resistance to the host nitrogen immune response. *Sci Rep.* 2016; 6:29349. <https://doi.org/10.1038/srep29349> PMID: 27435260
19. Tran SL, Guillemet E, Gohar M, Lereclus D, Ramarao N. CwpFM (EntFM) is a *Bacillus cereus* potential cell wall peptidase implicated in adhesion, biofilm formation and virulence. *J Bacteriol.* 2010; 192:2638–42. <https://doi.org/10.1128/JB.01315-09> PMID: 20233921
20. Tran SL, Guillemet E, Ngo-Camus M, Clybouv C, Puhar A, Moris A, et al. Hemolysin II is a *Bacillus cereus* virulence factor that induces apoptosis of macrophages. *Cell Microbiol.* 2011; 13:92–108. <https://doi.org/10.1111/j.1462-5822.2010.01522.x> PMID: 20731668
21. Tran SL, Cormontagne D, Vidic J, Andre-Leroux G, Ramarao N. Structural Modeling of Cell Wall Peptidase CwpFM (EntFM) Reveals Distinct Intrinsically Disordered Extensions Specific to Pathogenic *Bacillus cereus* Strains. *Toxins (Basel).* 2020; 12(9). <https://doi.org/10.3390/toxins12090593> PMID: 32937845
22. Glasset B, Herbin S, Granier S, Cavalié L, Lafeuille E, Guérin C, et al. *Bacillus cereus*, a serious cause of nosocomial infections: epidemiologic and genetic survey. *PLoS ONE.* 2018; 13(5):e0194346. <https://doi.org/10.1371/journal.pone.0194346> PMID: 29791442
23. Guinebretière MH, Broussolle V, Nguyen-The C. Enterotoxigenic profiles of food-poisoning and food-borne *Bacillus cereus* strains. *J Clin Microbiol.* 2002; 40(8):3053–6. <https://doi.org/10.1128/JCM.40.8.3053-3056.2002> PMID: 12149378
24. Martinez-Blanch JF, Sanchez G, Garay E, Aznar R. Development of a real-time PCR assay for detection and quantification of enterotoxigenic members of *Bacillus cereus* group in food samples. *Int J Food Microbiol.* 2009; 135(1):15–21. <https://doi.org/10.1016/j.ijfoodmicro.2009.07.013> PMID: 19665814
25. Kamar R, Gohar M, Jéhanno I, Réjasse A, Kallassy M, Lereclus D, et al. Pathogenic Potential of *Bacillus cereus* Strains as Revealed by Phenotypic Analysis. *J Clin Microbiol.* 2013; 51:320–3. <https://doi.org/10.1128/JCM.02848-12> PMID: 23135929
26. Kavanaugh D, Glasset B, Dervyn R, Guérin C, Plancade S, Cormontagne D, et al. New genetic biomarkers to differentiate pathogenic and clinically relevant *Bacillus cereus* strains. *Clin Microb Infect.* 2021. 7:S1198-743X(21)00283-4. <https://doi.org/10.1016/j.cmi.2021.05.035> PMID: 34111580
27. Dervyn R, Kavanaugh DW, Cormontagne D, Glasset B, Ramarao N. Identification of a new pathogenicity island within the large pAH187_270 plasmid involved in *Bacillus cereus* virulence. *Front. Cell. Infect. Microbiol.* 2021; 11:788757.
28. Callejas-Negrete OA, Torres-Guzman JC, Padilla-Guerrero IE, Esquivel-Naranjo U, Padilla-Ballesteros MF, Garcia-Tapia A, et al. The Adh1 gene of the fungus *Metarhizium anisopliae* is expressed during insect colonization and required for full virulence. *Microbiol Res.* 2015; 172:57–67. <https://doi.org/10.1016/j.micres.2014.11.006> PMID: 25534970
29. Saliola M, Falcone C. Two mitochondrial alcohol dehydrogenase activities of *Kluyveromyces lactis* are differently expressed during respiration and fermentation. *Mol Gen Genet.* 1995; 249(6):665–72. <https://doi.org/10.1007/BF00418036> PMID: 8544832
30. Kelly JM, Drysdale MR, Sealy-Lewis HM, Jones IG, Lockington RA. Alcohol dehydrogenase III in *Aspergillus nidulans* is anaerobically induced and post-transcriptionally regulated. *Mol Gen Genet.* 1990; 222(2–3):323–8. <https://doi.org/10.1007/BF00633836> PMID: 2274033
31. Bakker BM, Bro C, Kotter P, Luttk MA, van Dijken JP, Pronk JT. The mitochondrial alcohol dehydrogenase Adh3p is involved in a redox shuttle in *Saccharomyces cerevisiae*. *J Bacteriol.* 2000; 182(17):4730–7. <https://doi.org/10.1128/JB.182.17.4730-4737.2000> PMID: 10940011
32. Arnaud M, Chastanet A, Debarbouille M. New vector for efficient allelic replacement in naturally non-transformable, low-GC-content, gram-positive bacteria. *Appl Environ Microbiol.* 2004; 70(11):6887–91. <https://doi.org/10.1128/AEM.70.11.6887-6891.2004> PMID: 15528558
33. Hagan CT, Medik YB, Wang AZ. Nanotechnology Approaches to Improving Cancer Immunotherapy. *Adv Cancer Res.* 2018; 139:35–56. <https://doi.org/10.1016/bs.acr.2018.05.003> PMID: 29941106
34. Ramarao N, Nielsen-LeRoux C, Lereclus D. The insect *Galleria mellonella* as a powerful infection model to investigate bacterial pathogenesis. *J Vis Exp.* 2012; 70:e4392. <https://doi.org/10.3791/4392> PMID: 23271509

35. Tran S, Guillemet E, Lereclus D, Ramarao N. Iron regulates *Bacillus thuringiensis* haemolysin hlyII gene expression during insect infection. *J Invert Pathol*. 2013; 113:205–8. <https://doi.org/10.1016/j.jip.2013.04.001> PMID: 23598183
36. Murzin AG. Structural classification of proteins: new superfamilies. *Curr Opin Struct Biol*. 1996; 6(3):386–94. [https://doi.org/10.1016/s0959-440x\(96\)80059-5](https://doi.org/10.1016/s0959-440x(96)80059-5) PMID: 8804825
37. Taneja B, Mande SC. Conserved structural features and sequence patterns in the GroES fold family. *Protein Eng*. 1999; 12(10):815–8. <https://doi.org/10.1093/protein/12.10.815> PMID: 10556240
38. Rubach JK, Plapp BV. Amino acid residues in the nicotinamide binding site contribute to catalysis by horse liver alcohol dehydrogenase. *Biochemistry*. 2003; 42(10):2907–15. <https://doi.org/10.1021/bi0272656> PMID: 12627956
39. Thorn JM, Barton JD, Dixon NE, Ollis DL, Edwards KJ. Crystal structure of *Escherichia coli* QOR quinone oxidoreductase complexed with NADPH. *J Mol Biol*. 1995; 249(4):785–99. <https://doi.org/10.1006/jmbi.1995.0337> PMID: 7602590
40. Mukherjee PK, Mohamed S, Chandra J, Kuhn D, Liu S, Antar OS, et al. Alcohol dehydrogenase restricts the ability of the pathogen *Candida albicans* to form a biofilm on catheter surfaces through an ethanol-based mechanism. *Infect Immun*. 2006; 74(7):3804–16. <https://doi.org/10.1128/IAI.00161-06> PMID: 16790752
41. Plapp BV, Leidal KG, Murch BP, Green DW. Contribution of liver alcohol dehydrogenase to metabolism of alcohols in rats. *Chem Biol Interact*. 2015; 234:85–95. <https://doi.org/10.1016/j.cbi.2014.12.040> PMID: 25641189
42. Jornvall H, Persson B, Jeffery J. Characteristics of alcohol/polyol dehydrogenases. The zinc-containing long-chain alcohol dehydrogenases. *Eur J Biochem*. 1987; 167(2):195–201. <https://doi.org/10.1111/j.1432-1033.1987.tb13323.x> PMID: 3622514
43. Sun HW, Plapp BV. Progressive sequence alignment and molecular evolution of the Zn-containing alcohol dehydrogenase family. *J Mol Evol*. 1992; 34(6):522–35. <https://doi.org/10.1007/BF00160465> PMID: 1593644
44. Cadot C, Tran SL, Vignaud ML, De Buyser ML, Kolsto AB, Brisabois A, et al. InhA1, NprA and HlyII as candidates to differentiate pathogenic from non-pathogenic *Bacillus cereus* strains. *J Clin Microbiol*. 2010; 48:1358–65. <https://doi.org/10.1128/JCM.02123-09> PMID: 20129969
45. Tran SL, Ramarao N. *Bacillus cereus* immune escape: a journey within macrophages. *FEMS Microbiol Lett*. 2013; 347:1–6. <https://doi.org/10.1111/1574-6968.12209> PMID: 23827020
46. Porrini C, Ramarao N, Tran SL. Dr. NO and Mr. Toxic—the versatile role of nitric oxide. *Biol Chem*. 2020; 401(5):547–72. <https://doi.org/10.1515/hsz-2019-0368> PMID: 31811798
47. Chin MP, Schauer DB, Deen WM. Nitric oxide, oxygen, and superoxide formation and consumption in macrophages and colonic epithelial cells. *Chem Res Toxicol*. 2010; 23(4):778–87. <https://doi.org/10.1021/tx900415k> PMID: 20201482
48. Zaki MH, Akuta T, Akaike T. Nitric oxide-induced nitrate stress involved in microbial pathogenesis. *J Pharmacol Sci*. 2005; 98(2):117–29. <https://doi.org/10.1254/jphs.crj05004x> PMID: 15937405
49. Porrini C, Guérin C, Tran SL, Dervyn R, Nicolas P, Ramarao N. Implication of a Key Region of Six *Bacillus cereus* Genes Involved in Siroheme Synthesis, Nitrite Reductase Production and Iron Cluster Repair in the Bacterial Response to Nitric Oxide Stress. *Int J Mol Sci*. 2021; 11; 22(10):5079. <https://doi.org/10.3390/ijms22105079> PMID: 34064887
50. Madeira JP, Alpha-Bazin B, Armengaud J, Duport C. Time dynamics of the *Bacillus cereus* exoproteome are shaped by cellular oxidation. *Front Microbiol*. 2015; 6:342. <https://doi.org/10.3389/fmicb.2015.00342> PMID: 25954265
51. Agledal L, Niere M, Ziegler M. The phosphate makes a difference: cellular functions of NADP. *Redox Rep*. 2010; 15(1):2–10. <https://doi.org/10.1179/174329210X12650506623122> PMID: 20196923
52. Duport C, Jobin M, Schmitt P. Adaptation in *Bacillus cereus*: From Stress to Disease. *Front Microbiol*. 2016; 7:1550. <https://doi.org/10.3389/fmicb.2016.01550> PMID: 27757102
53. Leclerc M, Bedu-Ferrari C, Etienne-Mesmin L, Mariadassou M, Lebrouilly L, Tran SL, et al. Nitric Oxide Impacts Human Gut Microbiota Diversity and Functionalities. *mSystems*. 2021 Oct 26; 6(5):e0055821. <https://doi.org/10.1128/mSystems.00558-21> PMID: 34519530